Amplifier Nonlinear Modeling with RF Pulses

Carlos Crespo-Cadenas, *Associate, IEEE,* Javier Reina-Tosina, *Associate, IEEE,*
and María J. Madero-Ayora, *Student Member, IEEE*

***Abstract*—This paper proposes a Volterra kernel identification procedure for wireless amplifiers with nonlinear memory. The technique is based on a reduced-order model for wideband amplifiers (VBW) that is favorably compared with widely used memory polynomial model in terms of NMSE. The identification method takes advantage of the particular model structure and is thoroughly derived with a proper selection of pulse-like waveforms of known amplitude as probing signals, with special emphasis on the extraction of the fifth-order kernel. The main advantage of the method is that it allows exploring the dynamic range of the amplifier without rising the temperature in the device or altering the biasing point. For validation purposes, a commercial amplifier has been characterized and the extracted kernels have been used to predict the response under WCDMA-like signals. In addition to the simplicity of the deterministic approach used in this extraction procedure, the agreement of the predicted responses with measurements was highly satisfactory in all cases and permitted the capture of phenomena that are due to nonlinear memory effects.**

***Index Terms*—System identification, behavioral models, power amplifiers, nonlinear memory effects.**

I. Introduction

THE establishment of the Third-Generation cellular systems and the imminent advent of the Fourth-Generation mobile systems have propelled the study of novel techniques in wireless communications. Unlike the older GSM technology, the new wireless systems need highly linear power amplifiers, and the characterization of their nonlinear effects is increasingly necessary. In the field of amplifier modeling, the Volterra series approach offers a methodical way to analyze nonlinear effects appearing in the wireless communications channel. Under this approximation, the amplifier is entirely characterized by the Volterra kernels, the multidimensional impulse responses of the nonlinear system, so that a complete description of the amplifier is achieved when its kernels are experimentally determined.

Among the several techniques that can be used to measure the Volterra kernels of finite order, the one proposed in [1] was formally presented for a continuous-time second-order system. The technique relies in a bilinear operator and according to this procedure, the system output is measured under two input conditions, with one impulse and with two impulses. By applying repeatedly this signal with different temporal separation between the two unit impulses, the corresponding outputs are used to compute the second-order Volterra kernel.

Manuscript received February 12, 2008; revised June 7, 2008. This work was supported by the Spanish National Board of Scientific and Technological Research (CICYT) within the project TEC2004-06451-C05-03, and by the Regional Government of Andalusia (CICE) under grant P07-TIC-02649.

The authors are with the Departamento de Teoría de la Señal y Comunicaciones, Escuela Superior de Ingenieros, Universidad de Sevilla, Spain. Tel: +34954487336, Fax: +34 954487341. E-mail: ccrespo@us.es, jreina@us.es, mjmadero@us.es.

Based on the previous continuous-time case, the concept of bi-impulse response of a quadratic Volterra filter was introduced in [2] as a formal tool able to describe the corresponding discrete-time bilinear operator. In the same work, sample applications to the design of quadratic filters for image processing were also presented. Although the procedure can be extended to higher-order, the method is practically valid only for second-order filters. For systems with order higher than two, the excessive cost in measurement complexity makes necessary the use of other techniques, like the employment of Wiener functionals together with the application of Gaussian time functions as sounding signals.

In a wireless communications context, different types of behavioral models have been thoroughly used to describe amplifiers, some of them revised in [3] and others published more recently [4]-[9]. Our interest in this paper is focused on Volterra baseband models with memory for which, as long as the nonlinear behavior must be accurately described, at least the inclusion of the fifth-order terms are necessary. The complexity of the expression for a fifth-order general Volterra model makes impractical the use of multiple impulses to measure the amplifier kernels. Alternate approaches have been presented: for example, a kernel estimation algorithm which is optimal in the least mean square error sense was derived for a bandpass nonlinearity in [10]. However, this is a demanding procedure as long as it requires computation of input-output statistics up to sixth order and evaluation of sixteen estimation formulae.

An immediate form to simplify the extraction process can be attained with a reduction in the filter structure of the model, subject to the constraint of accuracy. Of course, the elementary memoryless model is not an acceptable alternative if the dynamic behavior of the amplifier has to be taken into account. An option to maintain a reasonable complexity and at the same time take into account memory effects was introduced in [11], in which the structure of the Volterra kernels was truncated by considering only the diagonal terms. Although the use of this memory polynomial model has been frequently reported in the literature, there are no fundamental considerations for the exclusion of the out-of-diagonal terms in an actual Volterra model [12]. Other nearly diagonal models with a more general structure have been proposed [4]-[5], but the reduction of kernel coefficients that these models present is not sufficient to make practical the use of pulse-like signals. The knowledge of the transfer functions behavior in the frequency domain has been utilized in the demonstration of the Volterra behavioral model for wideband amplifiers introduced in [6]. For a fifth-order representation, the primitive five-dimensional problem is reduced to a quadratic filter in the new Volterra behavioral model. Based on this order-reduction the authors have explored

in this work the application of the bi-impulse response and the bilinear operator concepts to an experimental kernel estimation procedure for wireless communications amplifiers. Some of the advantages of the use of pulse-like waveforms as sounding signals are understood by recalling for example that modern ultra wideband (UWB) communication systems transmit RF pulses, and this procedure would extract the model parameters in experimental conditions resembling the typical amplifier operation. RF pulses are also especially appropriate when testing on-wafer devices with no heat-sink, a situation in which the standard methods could damage the amplifier. Finally, excitation with pulse-like signals makes possible a direct and very precise kernel extraction, minimizing the measurement errors generated in the experimental setup.

The main objective of the present work is to demonstrate a procedure to identify the parameters of a baseband nonlinear model using RF pulses as probing signals in wideband amplifier characterization. This paper is organized as follows. Section II contains a brief explanation of the Volterra model for wideband amplifiers, together with some definitions and related properties, and the justification of the underlying assumptions. Section III documents the detailed experimental procedure for kernel identification and description of the sounding signals. Section IV evaluates the proposed approach in two steps: first, the validity of the model itself is verified by comparing its performance with other widely used behavioral models, following a standard least-squares procedure for parameter extraction. Measured results and relevant comparisons are provided. The proposed experimental approach is subsequently applied to a commercial amplifier, and the kernels identified with pulse-like waveforms are used to predict the amplifier response to digitally-modulated signals. Finally, some conclusions are outlined in Section V.

II. Initial Discussion on the Amplifier Model

The system we are dealing with is a nonlinear amplifier of a wireless communications system, for which we consider biasing conditions and input signals that permit its study as a stable, time-isotropic and shift-invariant nonlinear system with finite memory. Let the schematic of Fig. 1 represent the baseband equivalent of a wideband RF amplifier. In that case, the output corresponding to the fundamental frequency zone can be described by a discrete-time Volterra model whose general expression can be written as

$$\begin{aligned} y(k) = &\sum_{q_1} h_1(q_1)x(k-q_1)+ \\ &+\sum_{\mathbf{q}_3} h_3(\mathbf{q}_3)x(k-q_1)x(k-q_2)x^*(k-q_3)+ \\ &+\sum_{\mathbf{q}_5} h_5(\mathbf{q}_5)x(k-q_1)x(k-q_2)x(k-q_3)\times \\ &\times x^*(k-q_4)x^*(k-q_5)+\cdots . \end{aligned} \quad (1)$$

In this equation, $x(k)$ and $y(k)$ are complex envelope samples of the input and output RF signals, respectively, $h_n(\mathbf{q}_n)$ represents the discrete Volterra kernels of order n and $\mathbf{q}_n$ is an n-dimensional vector composed of the integer-valued delays q_i $(i = 1, \cdots, n)$.

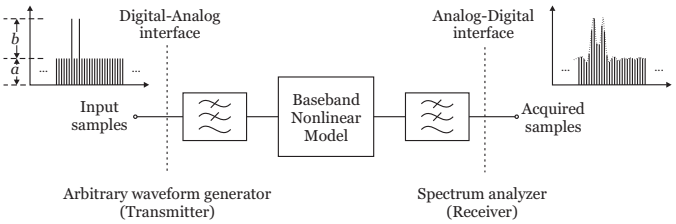

Fig. 1. Equivalent block diagram of the kernel identification setup.

This general Volterra model needs the realization of n filters with orders ranging from 1 to n and consequently presents the inconvenience of a high complexity, derived from the exorbitant number of coefficients necessary to describe the output. To overcome this drawback, several approaches for nonlinear amplifiers with memory have been advanced, many of them based on a static nonlinearity with input and/or output filters to incorporate linear memory (Wiener or Hammerstein models). In particular, Hammerstein-type schemes lead to kernels with a diagonal structure, a model that has been frequently reported in the literature [11], [13]. Nevertheless, the exclusion of the out-of-diagonal terms has not been theoretically demonstrated and other models with out-of-diagonal coefficients have been suggested [12], [5]. Beyond the ability to conform the empirical data, there are some basic notional questions not clarified by those proposed models. For example, the relation between the kernels and the amplifier nonlinear transfer functions or the invariability of these kernels with respect to a change in the type of probing signal, its input level or bandwidth, among others. Therefore, it is desirable the deduction of a Volterra model starting with the nonlinear transfer functions behavior at circuit level, in order to give response to the uncertainty on the kernel structure and to guarantee the kernels invariability.

A. Volterra Model for a Wideband RF Amplifier

The simplest description to be assumed is the behavioral memoryless model, based on the amplifier NLTF frequency independence. Recalling the narrowband condition ($B \ll f_c$), it is possible to assume a flat response at all frequency zones (about dc, the fundamental frequency and the other harmonics). The memoryless model fails when the signal bandwidth increases and the NLTFs can no longer be considered frequency-independent. However, as long as modern amplifiers have pass bands larger than the corresponding RF signal band, the wideband condition can be perfectly assumed for the linear response without important loss of generality. The extension of this condition is easily acceptable at all harmonic zones except at dc zone where the (even) NLTFs cannot be considered flat, because of the load impedance dependence on baseband frequency [14], [15]. The new Volterra model for wideband amplifiers (VBW) with nonlinear memory deduced in [6] is based on these assumptions and yields the following expression

$$y(k) = \left[h_1 + \sum_{m=1}^{\infty} \hat{h}_{2m+1}\left[|x(k)|^2\right] \right] x(k), \quad (2)$$

where we have used the operators $\hat{h}_{2m+1}[\cdot]$ defined as

$$\hat{h}_{2m+1}\left[|x(k)|^2\right] = \sum_{\mathbf{q}_m} h_{2m+1}(\mathbf{q}_m) \prod_{p=1}^{m} |x(k-q_p)|^2. \quad (3)$$

Notice the important complexity reduction accomplished by this model, for which the $(2m+1)$th-order term is computed with an mth-order Volterra filter.

The factor in brackets of (2) can be defined as the dynamic gain, i.e. the gain of the amplifier at instant k. Let $g(k)$ denote this dynamic gain

$$g(k) = h_1 + \sum_{m=1}^{\infty} \hat{h}_{2m+1}\left[|x(k)|^2\right], \quad (4)$$

and express the amplifier output in the form of the product of this gain by the input envelope $x(k)$, or

$$y(k) = g(k)x(k). \quad (5)$$

Observe that the dynamic gain contains all the memory of the model and is described by a Volterra filter whose input is the real-valued instantaneous power of the input envelope, $w(k) = |x(k)|^2$. Fig. 2 illustrates the resulting block diagram of the fifth-order model for a wideband RF amplifier, composed fundamentally by a linear filter and a homogeneous quadratic filter, which generate the gain according to the instantaneous input power.

One way to appreciate the accuracy of this model is by considering the influence of its most evident simplification, i.e. the frequency independence of the second-order NLTF. The consequence of this assumption is basically that the nonlinear memory effects are produced by variations of the input envelope magnitude, but they do not depend on the input envelope phase variations. The phase invariance of the VBW model is consistent with an actual fact: the existence of AM-AM and AM-PM conversion, but no PM-AM or PM-PM conversion. This general property has been exploited in mobile systems transmitting constant-amplitude RF signals with all the information contained in the phase: FM in analog systems and GMSK in the European GSM system.

In spite of the important order reduction, the VBW model is able to explain nonlinear memory effects or other related characteristics like spectrum asymmetry. This assertion can be clarified with a comparison with the model presented in Fig. 5 of [9], considering third-order terms to simplify the analysis. In that paper, the filter $G(\omega)$ plays a role similar to the linear filter of Fig. 2 with the difference that here the filter is composed by only one second-harmonic coefficient, because of the frequency-independence assumption, and it is incorporated to the corresponding baseband coefficient. Referring to the same paper, let emphasize that in the second-harmonic band the filter $G(\omega)$ presents a magnitude of approximately (6 ± 0.1) dB in the relevant band of 4 MHz (for the 2 MHz bandwidth of the experimental validating signal), or equivalently one percent of variation. This value is completely compatible with the assumption of a flat second-harmonic response. The inclusion of the probably complex-valued second-harmonic coefficient in the linear filter that describes the third-order term makes possible that the VBW model can represent intermodulation distortion asymmetry in nonlinear amplifiers as was experimentally demonstrated in [16].

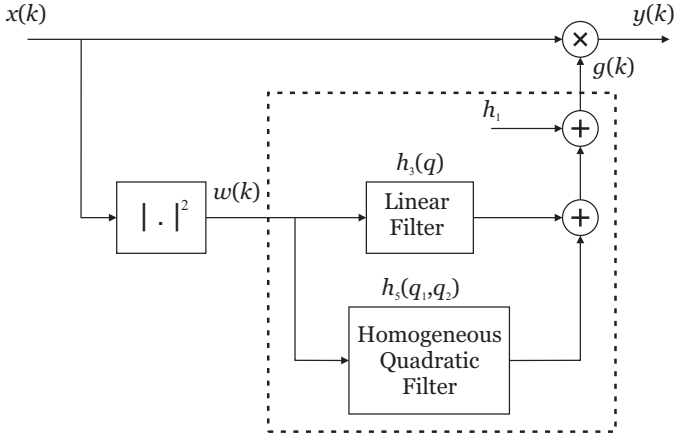

Fig. 2. Resulting block diagram for a fifth-order model of a wideband RF amplifier.

In addition to the previous remarks, we can also observe that the model is efficient predicting magnitude asymmetry if at least one of the even-order NLTFs is complex-valued, notwithstanding they are considered flat [14], [15]. In relation to this subject, notice that if the characteristic observed in an spectrum analyzer has (magnitude) asymmetry, then it is possible to say that the amplifier has memory, but the converse is not true. Even in the case of a spectrum with symmetric magnitude, it is possible to observe memory in an amplifier if its memory were related with phase asymmetry. It is worth to mention that as long as the utilization of wideband RF amplifiers is very common in wireless communications systems, it is reasonable to expect an ample application of these results without loss of precision even though the complexity reduction has been important.

B. Definitions

In addition to the dynamic gain, let us introduce some definitions.

1) Dynamic Gain Deviation: In general, the measured gain suffers deviations with respect to the small-signal gain caused by nonlinear distortion, measurement errors and noise. If the measurement errors and noise are negligible the dynamic gain deviation can be expressed by

$$d(k) = g(k) - h_1 = \hat{h}_3[w(k)] + \hat{h}_5[w(k)]. \quad (6)$$

Recalling that the input envelope is composed by two signals in quadrature, $x_I(k)$ and $x_Q(k)$, then the filter input is given by $w(k) = x_I^2(k) + x_Q^2(k) = w_I(k) + w_Q(k)$. It follows that the deviation is

$$d(k) = d_I(k) + d_Q(k) + d_{IQ}(k). \quad (7)$$

The terms

$$d_I(k) = \sum_{\mathbf{q}_1} h_3(\mathbf{q}_m) w_I(k-q_1) + \\ + \sum_{\mathbf{q}_2} h_5(\mathbf{q}_2) w_I(k-q_1) w_I(k-q_2) \quad (8)$$

and

$$d_Q(k) = \sum_{\mathbf{q}_1} h_3(\mathbf{q}_m) w_Q(k-q_1) + \\ + \sum_{\mathbf{q}_2} h_5(\mathbf{q}_2) w_Q(k-q_1) w_Q(k-q_2) \quad (9)$$

represent the deviations of the gain produced by the in-phase and quadrature signal components, respectively. The third term can be interpreted as the gain deviation produced by the simultaneous existence of in-phase and quadrature components in the input signal.

2) IQ-*Dynamic Gain Deviation:* This IQ-dynamic gain deviation is given by

$$d_{IQ}(k) = 2\hat{\hat{h}}_5\{w_I(k), w_Q(k)\}, \quad (10)$$

where

$$\hat{\hat{h}}_5\{w_I(k), w_Q(k)\} = \sum_{q_1,q_2=-Q_d/2}^{Q_d/2} h_5(q_1,q_2) w_I(k-q_1) w_Q(k-q_2) \quad (11)$$

is a bilinear operator [1], [2]. Without loss of generality, it has been assumed that Q_d is even and there is an index shift of $Q_d/2$ in the time reference. According to (7) and (10), the output of the bilinear operator can be expressed in terms of the acquired system outputs for three different inputs: the in-phase component $x_I(k)$, the quadrature component $x_Q(k)$ and the full complex envelope $x(k) = x_I(k) + jx_Q(k)$.

C. Properties of the Dynamic Gain Deviation

The dynamic gain deviation (6) presents some useful properties, summarized as follows:

- The dynamic gain deviation is phase invariant, i.e. it depends only on the envelope magnitude of the input signal.
- For any input signal scaled by a real-valued parameter α, the new envelope instantaneous power is $\alpha^2 w(k)$ and the dynamic gain deviation is given by $d(k) = \alpha^2 \hat{h}_3[w(k)] + \alpha^4 \hat{h}_5[w(k)]$.
- According to the previous property, if the input level is reduced 3 dB, then the new gain deviation is $d_{-3\text{dB}}(k) = \hat{h}_3[w(k)]/2 + \hat{h}_5[w(k)]/4$, and the difference $4d_{-3\text{dB}}(k) - d(k) = \hat{h}_3[w(k)]$ depends only on the third-order kernel.
- In the same form, the difference $d(k) - 2d_{-3\text{dB}}(k) = \hat{h}_5[w(k)]/2$ can be used as an indicator of the fifth-order terms significance.
- For signals satisfying the condition $x_I(k) = x_Q(k)$, the dynamic gain deviation is

$$d(k) = 2d_I(k) + d_{IQ}(k). \quad (12)$$

Considering that $d_I(k) = d_{-3\text{dB}}(k)$ and the IQ-gain deviation is $d_{IQ}(k) = d(k) - 2d_{-3\text{dB}}(k)$, the importance of fifth-order terms can be deduced from measurements at nominal level and at -3 dB.

III. Kernel Estimation Procedure

The order reduction exhibited by the VBW model allows to extract third- and fifth-order kernels by applying pulse-like signals. To identify the kernel elements up to the mth-order filter by applying a technique based on RF pulses it is necessary to evaluate the system response to a set of m distinct impulse waveforms. In the case of the second-order Volterra filter of the fifth-order VBW reduced model, parameter estimation is possible by evaluating its bi-impulse response, as demonstrated in [1] and [2]. The proposed technique can be divided into a first part in which the sounding signal is an RF pulse and provides the third-order coefficients, and a second part with two impulses at different temporal separation to extract the fifth-order coefficients. The complete procedure utilizes three sounding signals, designed as SS1 to SS3, which are described in the next subsections.

A. Third-order Kernel

To identify third-order kernel coefficients, the approach proposed in this paper makes use of the demonstrated properties of the dynamic gain deviation (6) in order to minimize the influence of higher-order terms in the extraction procedure. At this point it is also necessary to bear in mind that the laboratory setup used in our experiments requires a frequency reference so that a constant amplitude should be added to a pure "delta-like" input envelope. Alternatively, the use of phase locked instrumentation to do the measurements, would relax the need for a constant signal as a phase reference. In either forms the acquisition equipment can be synchronized to the nominal frequency and is able to detect adequately the variation of the output envelope. Let us consider the first sounding signal, used to identify the third-order kernel:

1) SS1. One RF pulse: If the input envelope components are selected as $x_I(k) = a + bu_0(k)$ and $x_Q(k) = 0$ where $u_0(k)$ is a unit impulse and $a, b > 0$, assuming a fifth-order model the difference $\Delta d(k) = 4d_{-3\text{dB}}(k) - d(k)$ is given by

$$\Delta d(k) = d^{(0)} + (2ab + b^2) h_3(k). \quad (13)$$

The first term on the right, $d^{(0)} = \bar{h}_{30} a^2$, can be extracted from the samples located apart several memory lengths, in the unmodulated part of the acquired signal. The second term directly gives the kernel coefficients, which can be estimated by following the next procedure:

1) Apply the RF pulse and measure the gain deviation at nominal level and at -3 dB.
2) Determine $d^{(0)}$ with the unmodulated part of the signal, selected according to the system memory.
3) Knowing a and b, use (13) to estimate the third-order kernel coefficients $h_3(k)$ for $k = -Q_d/2, \cdots, Q_d/2$.

B. Fifth-order Kernel

The most important properties of the two sounding signals employed in the identification process of the fifth-order kernel are described below. An extended exposition of the complete procedure is detailed the Appendix.

Identification of fifth-order kernel can be performed with the following two sounding signals:

2) SS2. One RF pulse with a constant component in quadrature: If the input envelope components are selected as $x_I(k) = a + bu_0(k)$ and $x_Q(k) = a$, it is possible to obtain the auxiliary variable

$$\Delta d^{(2)}(k) = d^{(2)}(k) - d_I^{(2)}(k) - d_Q^{(2)}(k) - d_{IQ}^{(0)}, \qquad (14)$$

where $d_{IQ}^{(0)} = 2\bar{h}_{50}a^4$ corresponds to the unmodulated part of the signal, $d_I^{(2)}(k)$ and $d_Q^{(2)}(k)$ are obtained with SS1 and the deviation $d^{(2)}(k)$ is measured directly.

3) SS3. Two RF pulses: If the input envelope components are selected as $x_I(k) = a + bu_0(k)$ and $x_Q(k) = a + bu_0(k - k_1)$ then the output of the bilinear operator is given by

$$d_{IQ}^{(3)}(k|k_1) = d_{IQ}^{(0)} + \Delta d^{(2)}(k) + \Delta d^{(2)}(k - k_1) + \\ + 2(2ab + b^2)^2 h_5(k, k - k_1). \qquad (15)$$

for $k = k_1 - Q_d/2, \cdots, k_1 + Q_d/2$. The term $d_{IQ}^{(3)}(k|k_1)$ denotes the IQ-deviation produced by the simultaneous presence of the two pulses separated k_1 samples.

According to (15) the fifth-order kernel coefficients can be estimated directly by measuring the deviation of two sounding signals and using the properties of the bilinear operator. The extraction procedure can be summarized as follows:

1) Apply the second sounding signal SS2, acquire the output and calculate the auxiliary term $\Delta d^{(2)}(k)$.
2) Acquire the output for the two RF pulses without temporal separation ($k_1 = 0$) at nominal level and with 3 dB reduction. Use a segment of unmodulated samples to determine $d_{IQ}^{(0)}$ and evaluate $\Delta d^{(2)}(k)$ from (14).
3) Estimate the diagonal coefficients $h_5(k, k)$ by evaluating (15).
4) Acquire the output for the two RF pulses with variable separation $k_1 = -Q_d/2, \cdots, Q_d/2$ and compute the remaining coefficients $h_5(k, k - k_1)$.

C. The Actual Sounding Signals

The procedure described above shows that for probing the amplifier it is only necessary the acquisition of Q_d+1 versions of a bi-impulse signal delayed k_1 samples. Some practical simplifications have been possible based on the particular symmetry of the pulses and also because the experimental setup used in this work permits acquisition lengths many times greater than the memory length of the amplifier. The overall acquisition length can be of 100 μs or approximately 1500 samples, very large compared to the conservative 20 samples of the device memory. Making use of this feature, the actual probing waveform was defined composed by three segments including the three types of signals described above. The normalized parameters for the RF pulses were chosen as $a = 1$ and $b = 4$, which are then scaled according to the input signal power level.

IV. Application to a Real RF Amplifier

To illustrate the present method, empirical extraction of kernels of a wireless wideband amplifier was performed. The experimental setup employed in this work was described in [16] and the device under test is a MAX2430 device (MAXIM Integrated Products Inc., Sunnyvale, CA), a silicon medium PA operating in the frequency range of 800-1000 MHz. A preliminary characterization with two-tones separated 2 MHz showed that the PA exhibited an asymmetry in the IMD products of about 5 dB, a clear indication of nonlinear memory effects. Power level was adjusted up to -10 dBm to enhance fifth-order effects. The arbitrary waveform facility of a SMIQ02B generator was used to define the I and Q components of the input envelope as a constant value plus unitary impulses at a sampling frequency of 15 Msa/s. These discrete-time signals are translated to narrow pulses in the continuous-time domain and to the corresponding RF pulses. The total length of the signal was 1500 samples, what allows the complete acquisition of the signal in an E4407B spectrum analyzer with the modulation analysis option. In that communication the authors described the extraction procedure of the third-order kernel, demonstrating the ability of the model to predict the amplifier output and its consistence for different experimental conditions. In this work we have developed the experimental setup used in the extraction technique incorporating several improvements in both the measurement techniques and processing of the acquisitions following some suggestions published in [17].

A. On the performance of the VBW model

As a previous step towards the validation of the kernel identification procedure presented herewith, an evaluation of the VBW model has been accomplished in order to demonstrate its good capabilities for the behavioral modeling of RF amplifiers.

The amplifier under test has been driven with a WCDMA-like signal at -14 and -10 dBm and kernel coefficients have been identified by using a conventional least-squares technique. The normalized mean square error (NMSE) between the measured waveform and the predicted signal corresponding to maximum delays in the range of 1 to 5 is depicted in Fig. 3. As a reference, results are compared with the memory polinomial (MP) model of the same order [11]. It is evident that VBW shows an improvement over the MP model, and that the comparison is even better when the amplifier is driven more nonlinearly.

As a cross-validation, kernels identified in the experiments of Fig. 3 were applied to predict the response of the amplifier at -14 dBm under different excitations, including pulse-like, GMSK-like, and other WCDMA-like signals, obtaining NMSEs in the range of -28 to -30 dB in all cases. The performance of VBW was comparable to that of the behavioral model recently published in [8] even though the number of coefficients of the VBW is considerably lower.

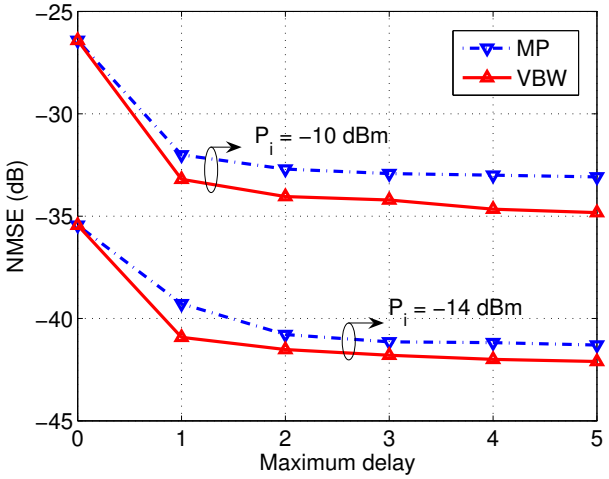

Fig. 3. Comparison of the VBW model and a fifth-order memory polinomial model.

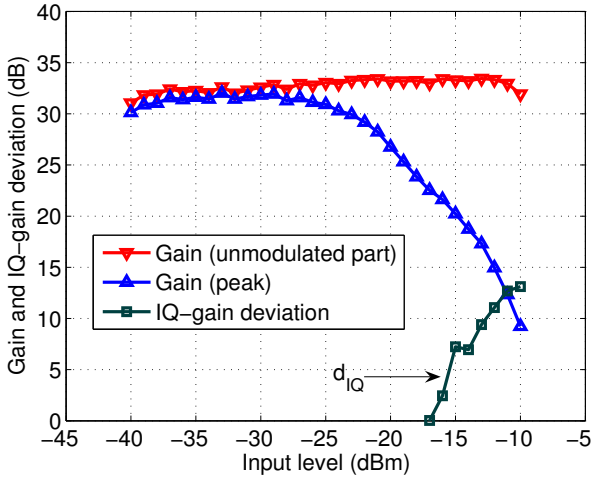

Fig. 4. Dynamic gain and IQ-gain deviation of the amplifier output with the first sounding signal.

B. Validation of the identification procedure

Based on the previous experience on third-order kernel extraction with RF pulses and using the concept of the aforementioned bi-impulse response, we have focused here on the fifth-order kernel estimation procedure. One important question to be solved is, given the model order, the range of power levels for which it is valid. For our test amplifier, it is possible to observe in Fig. 4 the gain corresponding to the unmodulated part of the first sounding signal, represented with down-triangles, as well as the gain measured at the instant corresponding to the peak, represented with up-triangles. It is clearly observable the larger compression, or equivalently the larger gain deviation, suffered by the peak compared to the unmodulated samples, especially for input signal levels above -20 dBm. In the same figure it is plotted the output of the bilinear operator d_{IQ} which is an indication of the fifth-order terms significance, as can be deduced from (10). In Fig. 5 a three-dimensional view of $h_3(q)$ is plotted as a function of the delays and the input signal power, in which the x-axis (depth) represents the input signal level, the y-axis (width) represents the delays and the z-axis (height) represents the magnitude of the kernel. The figure clearly shows the effective length of the memory, no more than six samples, and the practically constant characteristic of the memoryless coefficient with respect to the input signal level. This constant characteristic produces an increment of 3 dB per dB for the third-order output terms, as it should be. Observe that only at large signal levels the kernel coefficients are important with respect to measurement error and the extraction procedure is manifestly appropriate.

For a reliable extraction of the fifth-order kernel coefficients it is necessary to apply an adequate signal level in order to produce nonlinear terms well above other spurious responses due to noise or experimental errors. Recalling Fig. 4, it is observed that the output of the bilinear operator d_{IQ} is significant above -15 dBm, approximately. According to this result, the extraction of $h_5(q_1, q_2)$ coefficients was performed for an input level of -12 dBm and has been represented in

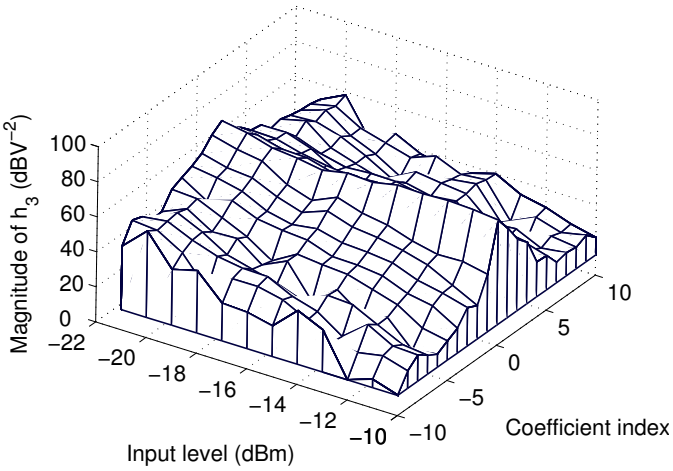

Fig. 5. Three-dimensional graph of the third-order kernel.

the three-dimensional graph of Fig. 6. The structure of the matrix is more clearly depicted in Fig. 7, in which the bright zones indicate the loci where the most significant components are concentrated. It is distinctly observable the more important central delay and the symmetry of the matrix with respect to the main diagonal. According to this figure, the diagonal terms are important near the center, but there are also relevant terms out of this main diagonal.

The amplifier was finally tested by employing a digitally modulated signal with a WCDMA format and a 2 Msymb/s train of symbols using root-raised cosine pulses. The input signal level was fixed at -12 dBm, for which the amplifier is markedly in nonlinear operation, and the samples acquired with the testbed are shown in Fig. 8 with marks. The kernels of the fifth-order model, obtained following the previous procedure, were used to predict the output signal and the results are represented in the same figure with solid lines. The high coincidence is confirmed by an NMSE of -29.4 dB. The linear and the third-order models are also plotted in dotted and

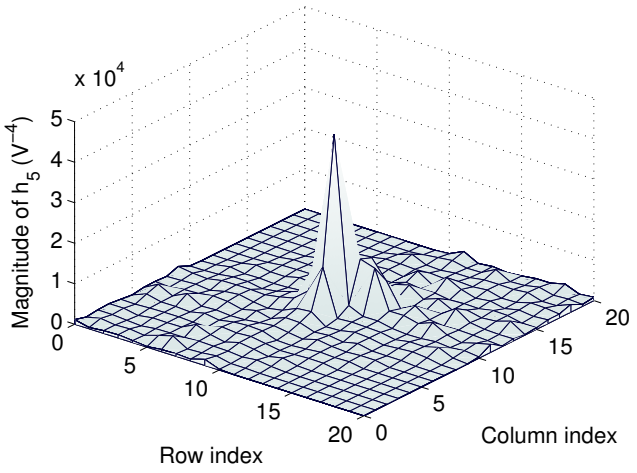

Fig. 6. Three-dimensional graph of the fifth-order kernel with 21×21 coefficients.

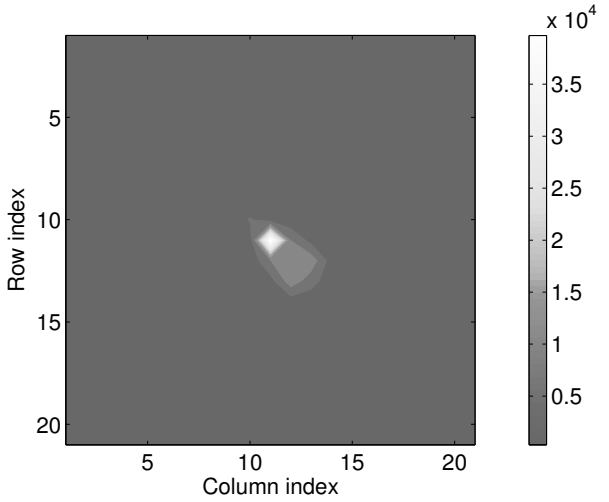

Fig. 7. Graphical representation of the fifth-order kernel matrix. A gray scale has been used with white color for more significant elements.

dash-dotted line, respectively. The figure demonstrates the high coincidence between the fifth-order model prediction and the measured data. This can also be observed in Fig. 9, where the power spectrum of the amplifier output measured with a standard spectrum analyzer is plotted with dots. The spectrum of the output calculated with the fifth-order model is represented in solid line and to give an idea of spectral regrowth, the spectrum of the linear model is also plotted in dotted line. The data obtained with the fifth-order VBW model are in agreement with the experimental data and, in consequence, reproduce adequately the asymmetry in the spectral content corresponding to the upper and lower adjacent channels. A numerical evidence of this assertion is contained in Table I, which shows the values of the power in the channel together with first- and second-adjacent channels powers calculated from the spectra of Fig. 9. It is important to note that these results were not obtained by following a mathematical curve-fitting procedure but using the described extraction technique based on RF bursts for kernels measurement and the application of these kernels to the digitally modulated signal. Although very different types of signals were used, the method and the model have produced very good estimates.

TABLE I
CHANNEL POWER AND ACP FOR A WCDMA-LIKE SIGNAL AT 2 MSPS.

Units: dBm	Co-channel power	1st Adjacent channel		2nd Adjacent channel	
		Lower	Upper	Lower	Upper
Measurements	20.1	-12.6	-8.1	-28.0	-32.6
Memoryless	20.1	-10.4	-10.4	-30.2	-30.2
VBW (5th-order)	20.1	-13.2	-8.2	-32.3	-37.4

V. CONCLUSIONS

This paper has reported on the use of the bi-impulse response to the process of model identification for wireless amplifiers. The technical procedure is based on the Volterra behavioral model for wideband amplifiers (VBW), which presents a significant complexity reduction. The assumptions in which the theoretical derivation of this behavioral model are based, have been clarified by obtaining NMSE figures in the order of -42 dB for the modeled output of a commercial amplifier excited by a WCDMA-like signal. These values outperform the results obtained with the widely accepted memory polynomial model, demonstrating the ability of VBW model to predict the amplifier output with a high precision.

According to the VBW model structure, a fifth-order amplifier model can be reduced to a quadratic filter and this reduction has made possible the development of a simple extraction technique in which the bilinear operator concept is applied to an experimental kernel estimation procedure. The use of pulse-like signals is not uncommon in device characterization, as in transistor dc or large-signal s-parameters measurements, but to the authors' knowledge it is the first time that pulsed waveforms are applied to the identification of behavioral models. With respect to other methods, using RF pulses as probing signals permits the exploration of the dynamic range of the amplifier without altering the dc bias point and the device temperature, a property that is related to the possibility of modeling UWB amplifiers with the same type of signal used in normal operation or on-wafer amplifiers without heat-sink. Moreover, RF pulses exhibit the valuable attribute of a flat-wideband spectrum.

The proposed identification procedure has relied on a careful signal processing aimed at the reduction of errors and the removal of linear filtering effects introduced by the experimental setup. As a consequence, in the process of model validation with a real amplifier working in a clear nonlinear operation and exhibiting memory effects, results show unequivocally the structure of the nonlinear kernels, obtaining NMSE values in the order of $-24/-29$ dB, with signals of different types.

The extracted kernels have been employed with very satisfactory results in the prediction of the output signal envelope, spectral regrowth, and ACPR of the amplifier under test excited by WCDMA-like signals.

The procedure presented in this paper does not put the

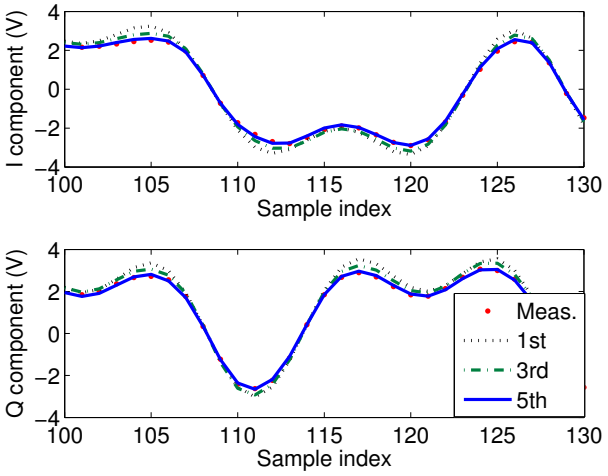

Fig. 8. Output waveform measured (marks) and predicted with a fifth-order model (solid line) for a WCDMA-like signal at −12 dBm. NMSE=−29.4 dB. The linear model is represented in dots and the third-order model in dash-dotted line.

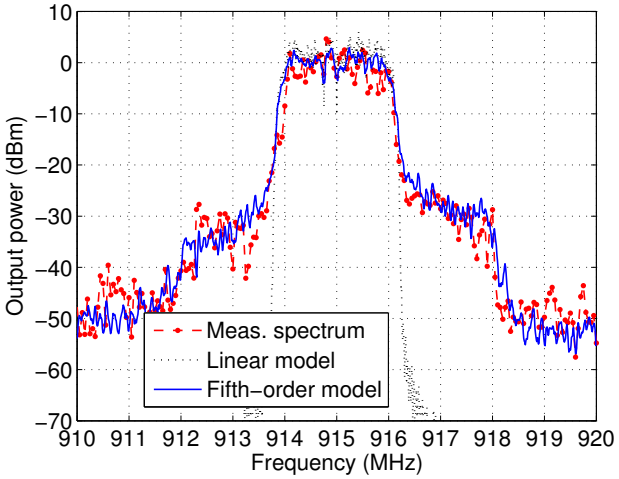

Fig. 9. Measured output spectrum trace of a WCDMA-like signal (marks) at −12 dBm and predicted with a fifth-order model (solid line). The predicted spectrum is also represented for the linear model(dotted line). Resolution bandwidth: 100 kHz.

finishing touches to the use of RF pulses. On the contrary, it is possible to anticipate the use of pulse-like signals with varying peak-amplitudes or signals with synchronized dc and RF pulses as an important help in the study of electrothermal causes for memory effects or, in the case of on-wafer devices without heat-sink, making possible the extraction of information highly correlated with the kernels values found under real operation.

APPENDIX

Further details follow about the sounding signals used for the identification of the fifth-order kernel and the extraction procedure:

1) SS2. One RF pulse with a constant component in quadrature: Using the bilinear operator, under excitation with envelope components $x_I(k) = a + bu_0(k)$ and $x_Q(k) = a$, the IQ-deviation is given by

$$d_{IQ}^{(2)}(k) = d_{IQ}^{(0)} + 2(2ab + b^2)a^2\bar{h}_{51}(k), \tag{16}$$

for $k = -Q_d/2, \cdots, Q_d/2$. We have used the constant IQ-deviation $d_{IQ}^{(0)} = 2\bar{h}_{50}a^4$ corresponding to the unmodulated part of the signal, as well as the definitions

$$\bar{h}_{50} = \sum_{q_1,q_2=-Q_d/2}^{Q_d/2} h_5(q_1, q_2) \tag{17}$$

and

$$\bar{h}_{51}(k) = \sum_{q_2=-Q_d/2}^{Q_d/2} h_5(k, q_2). \tag{18}$$

The deviation produced by the in-phase component, $d_I^{(2)}(k)$, is equal to the deviation of the first signal. The deviation of the quadrature component $d_Q^{(2)}(k)$ is equivalent to the overall deviation measured for the unmodulated segment of the second signal, but with a 3-dB level reduction. If the total deviation $d^{(2)}(k)$ is measured, then it is possible to express

$$d^{(2)}(k) - d_I^{(2)}(k) - d_Q^{(2)}(k) - d_{IQ}^{(0)} = \Delta d^{(2)}(k), \tag{19}$$

where $\Delta d^{(2)}(k) = 2(2ab + b^2)a^2\bar{h}_{51}(k)$.

2) SS3. Two RF pulses: If the input envelope components are selected as $x_I(k) = a + bu_0(k)$ and $x_Q(k) = a + bu_0(k - k_1)$, let $d_{IQ}^{(3)}(k|k_1)$ denote the IQ-deviation produced by the simultaneous presence of two bursts shifted by k_1 samples. In that case the output of the bilinear operator is given by (15). We have used the symmetry property $h_5(q_1, q_2) = h_5(q_2, q_1)$. Note that for $k_1 = 0$, the third signal with a 3-dB level reduction and the first sounding signal are equivalent, consequently $d_I^{(2)}(k)$ and $d_Q^{(2)}(k)$ are equal to $d_{-3\text{dB}}^{(3)}(k|0)$ near the peak and in the unmodulated segment, respectively. In the same form, the deviations of the in-phase and quadrature components of the third sounding signal at nominal level are equal to $d_{-3\text{dB}}^{(3)}(k|0)$.

REFERENCES

[1] M. Schetzen, "Nonlinear Systems Modeling Based on the Wiener Theory," *Proc. IEEE*, vol. 69, no. 12, pp. 1557–1573, Dec. 1981.
[2] G. Ramponi, "Bi-Impulse Response Design of Isotropic Quadratic Filters," *Proc. IEEE*, vol. 78, no. 4, pp. 665–677, Apr. 1990.
[3] J. C. Pedro and S. A. Maas, "A Comparative Overview of Microwave and Wireless Power Amplifier Behavioral Approaches," *IEEE Trans. Microw. Theory Tech.*, vol. 53, no. 4, pp. 1150–1163, Dec. 2005.
[4] D. R. Morgan, Z. Ma, J. Kim, M. G. Zierdt, and J. Pastalan, "A Generalized Memory Polynomial Model for Digital Predistortion of RF Power Amplifiers," *IEEE Trans. Signal Process.*, vol. 54, no. 10, pp. 3852–3860, Oct. 2006.
[5] A. Zhu, J. C. Pedro, and T. J. Brazil, "Dynamic Deviation Reduction-Based Volterra Behavioral Modeling of RF Power Amplifiers," *IEEE Trans. Microw. Theory Tech.*, vol. 54, no. 12, pp. 4323–4332, Dec. 2006.
[6] C. Crespo-Cadenas, J. Reina-Tosina, and M. J. Madero-Ayora, "Volterra Behavioral Model for Wideband RF Amplifiers," *IEEE Trans. Microw. Theory Tech.*, vol. 55, no. 3, pp. 449–457, Mar. 2007.
[7] A. Zhu, J. C. Pedro, and T. R. Cunha, "Pruning the Volterra Series for Behavioral Modeling of Power Amplifiers Using Physical Knowledge," *IEEE Trans. Microw. Theory Tech.*, vol. 55, no. 5, pp. 813–821, May 2007.

[8] D. Wisell and M. Isaksson, "Derivation of a Behavioral RF Power Amplifier Model with Low Normalized Mean-Square Error," in *Proc. 37th Eur. Microw. Conf.*, Munich, Germany, Oct. 2007, pp. 1283–1286.
[9] T. R. Cunha, J. C. Pedro, P. M. Cabral, "Design of a Power-Amplifier Feed-Forward RF Model With Physical Knowledge Considerations," *IEEE Trans. Microw. Theory Tech.*, vol. 55, no. 12, pp. 2747–2756, Dec. 2007.
[10] C. H. Cheng and E. J. Powers, "Optimal Volterra Kernel Estimation Algorithms for a Nonlinear Communication System for PSK and QAM Inputs," *IEEE Trans. Signal Process.*, vol. 49, no. 1, pp. 147–163, Jan. 2001.
[11] J. Kim and K. Konstantinou, "Digital predistortion of wideband signals based on power amplifier model with memory," *Electron. Lett.*, vol. 37, no. 23, pp. 1417–1418, Nov. 2001.
[12] A. Zhu and T. J. Brazil, "Behavioral Modeling of RF Power Amplifiers Based on Pruned Volterra Series," *IEEE Microw. Wireless Compon. Lett.*, vol. 14, no. 12, pp. 563–565, Dec. 2004.
[13] V. J. Mathews and G. L. Sicuranza, *Polynomial Signal Processing*, New York: Wiley, 2000.
[14] J. Brinkhoff and A. E. Parker, "Effect of baseband impedance on FET intermodulation," *IEEE Trans. Microw. Theory Tech.*, vol. 51, no. 3, pp. 1045–1051, Mar. 2003.
[15] C. Crespo-Cadenas, J. Reina-Tosina, and M. J. Madero-Ayora, "IM3 and IM5 phase characterization and analysis based on a simplified Newton approach," *IEEE Trans. Microw. Theory Tech.*, vol. 54, no. 1, pp. 321–328, Jan. 2006.
[16] C. Crespo-Cadenas, J. Reina-Tosina, and M. J. Madero-Ayora, "On the Use of RF Bursts for Identification of Amplifier Kernels," in *Proc. 37th Eur. Microw. Conf.*, Munich, Germany, Oct. 2007, pp. 1165–1168.
[17] M. Isaksson, D. Wisell and D. Ronnow, "A Comparative Analysis of Behavioral Models for RF Power Amplifiers," *IEEE Trans. Microw. Theory Tech.*, vol. 54, no. 1, pp. 348–359, Jan. 2006.

Carlos Crespo-Cadenas was born in Madrid, Spain. He received the degree in Physics in 1973 and Doctor degree in 1995 from the Polytechnique University of Madrid. Since 1998 he has been Associate Professor and currently he teaches lectures on Radio Communications in the Department of Signal Theory and Communications, University of Seville. His current interests are Nonlinear Analysis applied to Wireless Digital Communications and to Microwave Monolithic Integrated Circuits (MMIC).

Javier Reina-Tosina was born in Seville, Spain, in May 1973. He received the Telecommunication Engineering and Doctor degrees from the University of Seville, Seville, Spain, in 1996 and 2003, respectively. Since 1997 he has been with the Department of Signal Theory and Communications, University of Seville, where he is currently an Associate Professor. His research interests include MMIC technology, nonlinear analysis of active microwave devices and integration of information technologies in biomedicine.

María J. Madero-Ayora received the Telecommunication Engineering degree from the University of Seville, Seville, Spain, in 2002. Since 2003 she has been with the Department of Signal Theory and Communications, University of Seville, and is currently working toward the Doctor degree in Telecommunication Engineering. Her research interests focus on the area of nonlinear analysis of active microwave devices and measurement techniques for nonlinear communication systems.